Direct Calculation Method of Reference Flux Linkage for Maximum Torque per Ampere Control in DTC-Based IPMSM Drives

Atsushi Shinohara, *Student Member, IEEE*, Yukinori Inoue, *Member, IEEE*, Shigeo Morimoto, *Member, IEEE*, and Masayuki Sanada, *Member, IEEE*

***Abstract*—This paper proposes a maximum torque per ampere control strategy for direct-torque-controlled interior permanent magnet synchronous motor drives. The proposed method is based on the solutions of a quartic equation, a motor model in the *d-q* rotating frame often used for the synchronous motor controllers, and a well-known equation for maximum torque per ampere control. Therefore, the proposed method does not use a lookup table that depends on parameters of the motor and that has to be created in advance. In addition, the proposed method can use the estimated parameters. Particularly, the variations of the *d*- and *q*-axes inductances can be estimated when the inductances are modeled as the functions of the *d*- and *q*-axes current. The simulation results validate that the proposed method can achieve the maximum torque per ampere control. In addition, the simulation and experimental results verify the accuracy improvement of the maximum torque per ampere control with the iterated calculation.**

***Index Terms*—Direct torque control (DTC), maximum torque per ampere (MTPA), permanent magnet motors.**

I. Introduction

PERMANENT magnet synchronous motors (PMSMs) are widely used in various applications because of their several advantages, such as high power, high efficiency, and a wide operational speed range. Consequently, many researchers have investigated control strategies for realizing such attractive characteristics. Generally, *d*- and *q*-axes current control is used for high-performance motor drives, and many control laws are based on mathematical models in the *d-q* rotating frame, which is synchronized with the rotor.

Maximum torque per ampere (MTPA) control strategy is proposed as one of the current vector control strategies for high power and efficiency drives. The purpose of MTPA control strategy is to minimize copper loss, and this strategy is applied to low-speed ranges because the back electromotive force is small, and the voltage limitation can be neglected [1], [2]. The law of MTPA control strategy states the relationship of the *d*- and *q*-axes components of the armature current, making, MTPA control strategy suitable for current-control-based PMSM drives using *d-q* frame. There are several MTPA control strategies for current-control-based PMSM drives [3]–[9].

Direct torque control (DTC) was first proposed for induction motor drives [10]. DTC can be applied for all types of AC motors [11], [12], including PMSMs because DTC controls and estimates the stator flux linkage vector. DTC requires the electromagnetic torque and amplitude of the stator flux linkage as the references. On the other hand, DTC has no current control loop, and the current is not regulated directly [12]. As a result, it is difficult to control the current in DTC drives.

Few calculation methods for the reference flux linkage to realize MTPA control have already proposed for the synchronous reluctance motors [13], [14]. For the surface-mounted PMSMs, the reference stator flux linkage for MTPA control can be calculated easily to consider the case when *d*-axis current is zero. However, for the interior PMSMs (IPMSMs), the reference flux linkage for MTPA control is obtained using a lookup table (LUT), because the relationship between the torque and the stator flux linkage is more complex than the relationship between *d*- and *q*-axes currents. This relationship is influenced by the *d*- and *q*-axes inductances and the magnet flux linkage. In current-control-based IPMSM drives, MTPA control can be realized in advance without knowing the motor parameters through parameter estimation during operation [3], [4]. On the contrary, in DTC-based IPMSM drives, conventional MTPA control strategies require the knowledge of the motor parameters to create the LUT [11], [15]. Thus, it is difficult to apply the estimated parameters for MTPA control in DTC-based PMSM drives, and thus a reference flux linkage calculation method without an LUT is required for DTC-based IPMSM drive systems. In [16]–[18], the reference flux linkage is calculated according to the motor condition. However, convergence time is required to converge on the optimal reference flux linkage for MTPA control because the reference flux linkage depends on the motor condition, such as armature current.

This paper proposes a reference flux calculation method that realizes MTPA control in DTC-based IPMSM drives without the parameter-dependent LUT. This method is based on an IPMSM model and the relationship of MTPA control in the *d-q* frame [19]. The reference flux linkage can be calculated directly from the reference torque using mathematical formulae derived in this paper. Therefore, the reference flux linkage for MTPA control is independent of the motor condition, and there is less convergence time to obtain the optimal reference flux linkage. In addition, estimated inductance can be applied to the proposed

Manuscript received December 10, 2015; revised March 3, 2016; accepted May 8, 2016. Date of publication May 16, 2016; date of current version December 9, 2016. Recommended for publication by Associate Editor J. Zhang.

The authors are with the Osaka Prefecture University, Osaka 599-8531, Japan (e-mail: ss106030@edu.osakafu-u.ac.jp; inoue@eis.osakafu-u.ac.jp; morimoto@eis.osakafu-u.ac.jp; sanada@eis.osakafu-u.ac.jp).

Color versions of one or more of the figures in this paper are available online at http://ieeexplore.ieee.org.

Digital Object Identifier 10.1109/TPEL.2016.2569140

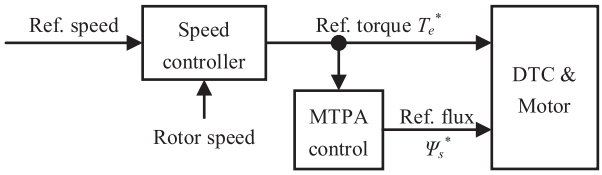

Fig. 1. Simplified block diagram of the DTC.

method. In this paper, modeled q-axis inductance as a function of the q-axis current is applied. This paper shows that the proposed method can realize the MTPA condition through simulations and that the proposed method can consider parameter variation with performing simulations and experiments using modeled q-axis inductance.

II. MTPA Control Strategy in DTC

A. Reference Calculator for DTC

Fig. 1 shows the block diagram of the DTC. Generally, a DTC system requires the torque T_e and stator flux linkage amplitude Ψ_s as its references. For the speed control system, the reference torque T_e^* is generated from the reference and actual (or estimated) rotor speeds. On the other hand, the reference flux linkage amplitude Ψ_s^* is generated from T_e^* for the MTPA control.

B. Equations for IPMSM in MTPA Condition

The equations for IPMSMs in the d-q frame are given by

$$T_e = P_n \{ \Psi_a - (L_q - L_d) i_d \} i_q \tag{1}$$

$$\begin{bmatrix} \Psi_d \\ \Psi_q \end{bmatrix} = \begin{bmatrix} \Psi_a + L_d i_d \\ L_q i_q \end{bmatrix} \tag{2}$$

where $\boldsymbol{i}_d$ and i_q are the d- and q-axes components of the armature current vector $\boldsymbol{i}_a$; Ψ_d and Ψ_q are the d- and q-axes components of the stator flux linkage vector Ψ_s; L_d and L_q are the d- and q-axes inductances; Ψ_a is the magnet flux linkage; and P_n is the number of pole pairs, respectively.

IPMSMs can use the reluctance torque, which depends on both d- and q-axes currents, because of their saliency. Therefore, the armature current vector is optimally controlled in order to produce maximum torque for a constant current. From (1), the relationship between i_d and i_q for MTPA control is derived as follows [2]:

$$i_d = \frac{\Psi_a}{2(L_q - L_d)} - \sqrt{\frac{\Psi_a^2}{4(L_q - L_d)^2} + i_q^2}. \tag{3}$$

In IPMSMs, i_d cannot be positive because L_q is larger than L_d.

This relationship can be rewritten as shown in

$$(L_q - L_d)^2 i_q^2 = \Psi_D \left(\Psi_D - \Psi_a \right) \tag{4}$$

where

$$\Psi_D = \Psi_a - (L_q - L_d) i_d. \tag{5}$$

During MTPA control, Ψ_D is larger than Ψ_a because i_d is smaller than 0 and L_q is larger than L_d in IPMSMs. Moreover, Ψ_D is the same as the amplitude of "active flux" reported in [20].

On the other hand, Ψ_s can be calculated as follows:

$$\Psi_s^2 = \left(\Psi_a + L_d i_d \right)^2 + \left(L_q i_q \right)^2 . \tag{6}$$

C. Relationship Between Torque and Stator Flux Linkage

As described previously, the reference flux linkage is required to be calculated from the reference torque. However, the relationship of the MTPA control shown in (3) is unavailable directly in DTC because DTC requires the relationship between the torque and the stator flux linkage amplitude.

Here, by substituting (4) and (5) into (1) and (6), T_e and Ψ_s can be given as the function of Ψ_D, as follows:

$$\left(\frac{L_q - L_d}{P_n} T_e \right)^2 = \left(\Psi_D - \Psi_a \right) \Psi_D^3 \tag{7}$$

$$\Psi_{s\text{-}MTPA}^2 = \frac{\left(L_q^2 + L_d^2 \right) \Psi_D^2 - L_q \left(L_q + 2L_d \right) \Psi_a \Psi_D + L_q^2 \Psi_a^2}{(L_q - L_d)^2} \tag{8}$$

where $\Psi_{s\text{-}MTPA}$ is the stator flux linkage that satisfies (3).

Equations (7) and (8) are also described as follows:

$$\left(\frac{L_q - L_d}{P_n \Psi_a^2} T_e \right)^2 = (\gamma_D - 1) \gamma_D^3 \tag{9}$$

$$\Psi_{s\text{-}MTPA}^2 = \frac{\left(L_q^2 + L_d^2 \right) \gamma_D^2 - L_q \left(L_q + 2L_d \right) \gamma_D + L_q^2}{(L_q - L_d)^2} \Psi_a^2 \tag{10}$$

where γ_D is a nondimensional variable and is given by

$$\gamma_D = \Psi_D / \Psi_a . \tag{11}$$

Equation (9) is a quartic equation for γ_D. The four solutions of (9) are described as follows:

$$\gamma_D = \frac{(x_R + 1)}{4} \left(1 \pm \sqrt{\frac{2}{x_R} - 1} \right) \tag{12}$$

$$\gamma_D = \frac{(x_R - 1)}{4} \left(1 \pm \sqrt{-\frac{2}{x_R} - 1} \right) \tag{13}$$

where

$$x_R = \sqrt{\frac{1}{2} \left\{ \left(\sqrt{3x_T^2 + 1} + 1 \right)^{\frac{1}{3}} - \left(\sqrt{3x_T^2 + 1} - 1 \right)^{\frac{1}{3}} \right\}^3} \tag{14}$$

$$x_T = \frac{16(L_q - L_d)}{9 P_n \Psi_a^2} T_e \tag{15}$$

and x_R and x_T are also nondimensional variables.

Because both γ_D and the left-hand side of (9) must not have a negative value, the solutions of (9) can be limited to the

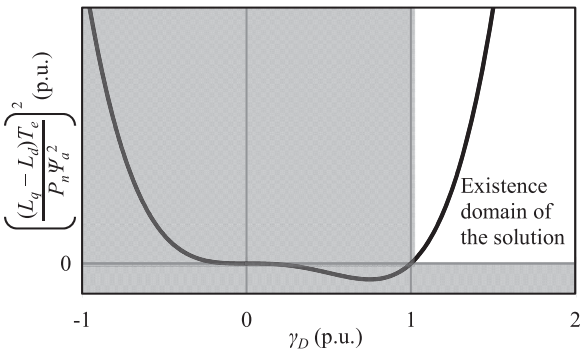

Fig. 2. Existence domain of (9).

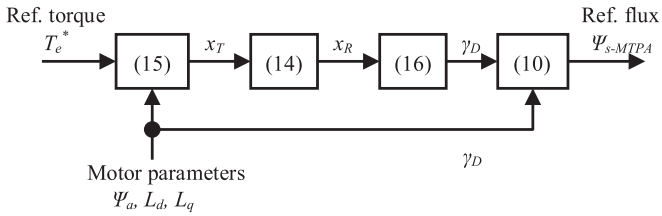

Fig. 3. Block diagram of the proposed reference flux linkage calculator for MTPA control.

following equation:

$$\gamma_D = \frac{(1+x_R)}{4}\left(1+\sqrt{\frac{2}{x_R}-1}\right). \tag{16}$$

Fig. 2 shows the existence domain of (9) in detail.

Fig. 3 shows the block diagram to calculate the reference flux linkage for the MTPA control. First, γ_D is calculated from the reference torque T_e^* using (14)–(16). Next, $\Psi_{s\text{-}MTPA}$ is calculated from γ_D using (10). Then, $\Psi_{s\text{-}MTPA}$ is applied to the reference flux linkage Ψ_s^*. The estimated motor parameters of IPMSMs can be easily applied to (10) and (15).

D. Considering Inductance Variation

Equation (3) assumes constant inductances but inductances vary because of magnetic saturation, causing the MTPA control point to move [5]. As described later, the optimal reference flux linkage varies with the inductance. Usually, the inductances are related to the current [2]–[7], [13], [17], [21]. In the proposed method, the *d*- and *q*-axes currents can be estimated from γ_D using (1), (5), and (11). Thus, the estimated *d*- and *q*-axes currents $\hat{i}_d$ and $\hat{i}_q$ can be described as

$$\hat{i}_d = \frac{\Psi_a}{L_d - L_q}(\gamma_D - 1) \tag{17}$$

$$\hat{i}_q = \frac{T_e^*}{P_n \Psi_a}\frac{1}{\gamma_D}. \tag{18}$$

When inductances are modeled as the function of currents, their value can be found using the estimated current. Fig. 4 shows the reference flux linkage calculation method that has a step for inductance estimation. First, γ_D is calculated with the initial values of the inductances. Next, the *d*- and *q*-axes currents are

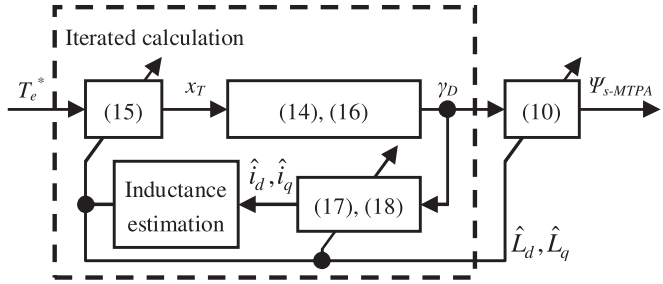

Fig. 4. Reference flux linkage calculator for MTPA control with iterated calculation and modeled inductances.

estimated from (17) and (18). After that, inductances are calculated from estimated current. Then, γ_D is calculated again with the estimated inductances. The reference flux linkage can get close to the reference value that satisfies MTPA condition with the iteration of calculating γ_D during the same control period.

Iterated calculation makes the reference flux linkage for MTPA control more accurate. In this way, measured values, such as armature current vector, are not required. However, the calculation load and times of iteration need to be considered. On the other hand, although i_d and i_q can be measured, the iterated calculation is better in adaptation to the torque changes.

III. Simulation Results

A. Tested System

DTC controls the stator flux linkage vector based on the following equation in the α-β stationary reference frame:

$$\frac{d\boldsymbol{\Psi}_\mathbf{s}}{dt} = \boldsymbol{v_a} - R_a \boldsymbol{i_a} = \boldsymbol{v_o} \tag{19}$$

where $\boldsymbol{v_a}$, $\boldsymbol{v_o}$, and $\boldsymbol{\Psi_s}$ are the armature voltage, induced voltage, and the stator flux linkage vectors, respectively, and R_a is the armature resistance.

The torque T_e can be calculated from outer product of the stator flux linkage and the armature current vectors:

$$T_e = P_n \boldsymbol{\Psi_s} \times \boldsymbol{i_a}. \tag{20}$$

Fig. 5 shows the tested IPMSM drive system. The system is based on the DTC using reference flux vector calculator (RFVC) [12], [13], [22]. The feature of this system is to use pulsewidth modulation (PWM) for the generation of the switching signal as well as current-control-based PMSM drives. T_s is the control period of DTC. Symbols with an asterisk represent the reference value in each variable.

In simulation, the flux estimator is structured as shown in Fig. 6, which is based on (19). In Fig. 6, *s* is the Laplace operator.

In the MTPA condition, the amplitude of armature current I_a is minimized under constant torque. Thus, to validate the MTPA condition, the relationship between Ψ_s^* and I_a is verified under constant load torque. In this paper, the reference flux linkage is set at the value obtained from the product of $\Psi_{s\text{-}MTPA}$ and correction rate ε as follows:

$$\Psi_s^* = \varepsilon \Psi_{s\text{-}MTPA}. \tag{21}$$

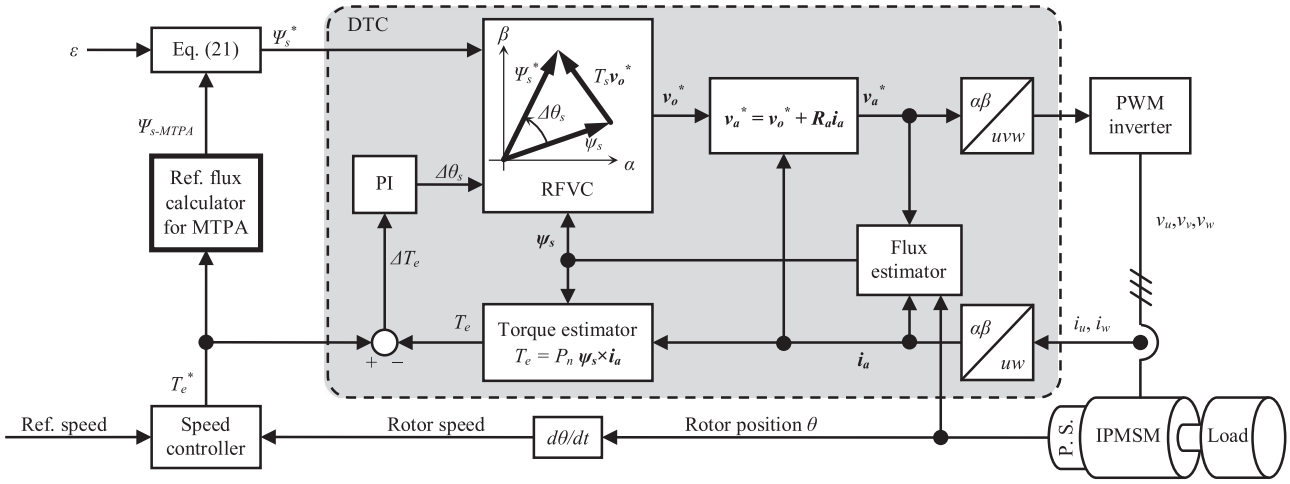

Fig. 5. Block diagram of the tested DTC system.

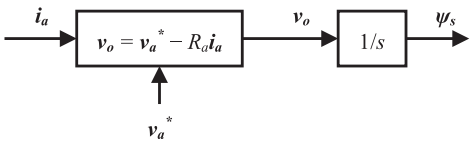

Fig. 6. Block diagram of the flux estimator in simulation.

TABLE I
PARAMETERS OF TESTED IPMSMS

Parameter characteristics	Motor 1	Motor 2
Number of pole pairs P_n	2	2
Armature resistance R_a	0.824 Ω	0.824 Ω
Magnet flux linkage Ψ_a	78.5 mWb	78.5 mWb
d-axis inductance L_d	9.67 mH	9.67 mH
q-axis inductance L_q	24.3 mH	$24.3 - 0.7\|i_q\|$ [mH]
Rated armature current	8.66 A	8.66 A
Rated torque	2.14 N · m	1.77 N · m

TABLE II
PARAMETERS OF CONTROLLER

Period of DTC T_s	100 μs
Period of reference calculator	5 ms
PWM carrier frequency	10 kHz
DC-link voltage	150 V
Limiting value of armature voltage	80 V
Limiting value of armature current	11 A

The variation of the reference flux linkage under constant reference torque can be expressed as the variation of ε. $\Psi_{s\text{-}MTPA}$ satisfies the reference flux linkage for MTPA control when I_a is minimized at $\varepsilon = 1$ under constant torque.

Table I lists the parameters of the two IPMSMs used in the simulations. Compared to Motor 1, Motor 2 has the variation of L_q as the function of i_q.

Table II shows the parameters in DTC. The proposed method is computed in a reference calculator with a control period of 5 ms.

B. Validation of MTPA Condition

In this section, it is verified that the proposed method satisfies MTPA condition. Motor 1 is applied to the tested system and the relationship between the amplitude of armature current I_a and the correction rate ε is evaluated under constant speed and load torque. Fig. 7 shows the relationship between I_a and ε. The rotor speed is 300 min^{-1}. In Fig. 7, I_a is minimum at $\varepsilon = 1$ in each torque. Thus, the proposed method satisfies MTPA condition in Motor 1 whose parameters are constant.

C. Transient State Characteristics

In this section, it is verified that the proposed method can also be adaptive in the transient state when Motor 1 is applied. The reference speed is changed from 200 to 2000 min^{-1} at 0.5 s. The reference torque T_e^* is limited to 2.2 N · m in the speed controller. To verify the proposed method, the correction rate ε is set at 0.8, 1.0, and 1.1. Fig. 8 shows the acceleration characteristics. Because of the limiting of the reference torque, the characteristics of the rotor speed the torque are very similar, as shown in Fig. 8(a). However, the characteristics of the armature current I_a are not similar because of the difference of the stator flux linkage as shown in Fig. 8(b) and (c). To compare three cases, the armature current is smallest when $\varepsilon = 1$ in any time.

Fig. 9 shows the relationship between the torque and the stator flux linkage under the transient state when $\varepsilon = 1$. The operating condition is the same as Fig. 8, and the relationship follows the MTPA curve on $\Psi_s - T_e$ plane. When the torque is changed at 0.5 s, the operating points deviate from MTPA curve in actual torque and actual stator flux linkage because of the difference in the response speed between the torque and the stator flux linkage. However, the operating points are fitted to MTPA curve every time, except for the actual value at 0.5 s. Moreover, the reference stator flux linkage is independent of motor condition because the operating points of the references follow MTPA curve every time as shown in Fig. 9(a).These results mean that $\Psi_{s\text{-}MTPA}$ with the proposed method can achieve MTPA control and that the proposed method is also effective in transient state.

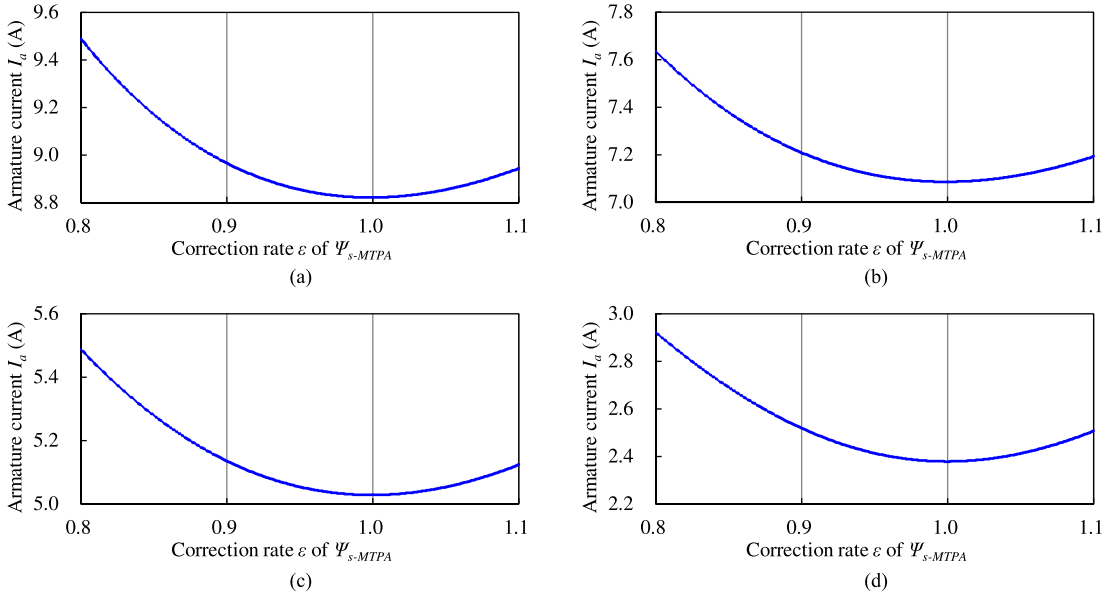

Fig. 7. Simulation results of the relationship between the armature current and the correction rate under the constant torque with Motor 1 at the rotor speed of 300 min^{-1}. (a) 2.2 N · m (rated), (b) 1.6 N · m, (c) 1.0 N · m, and (d) 0.4 N · m.

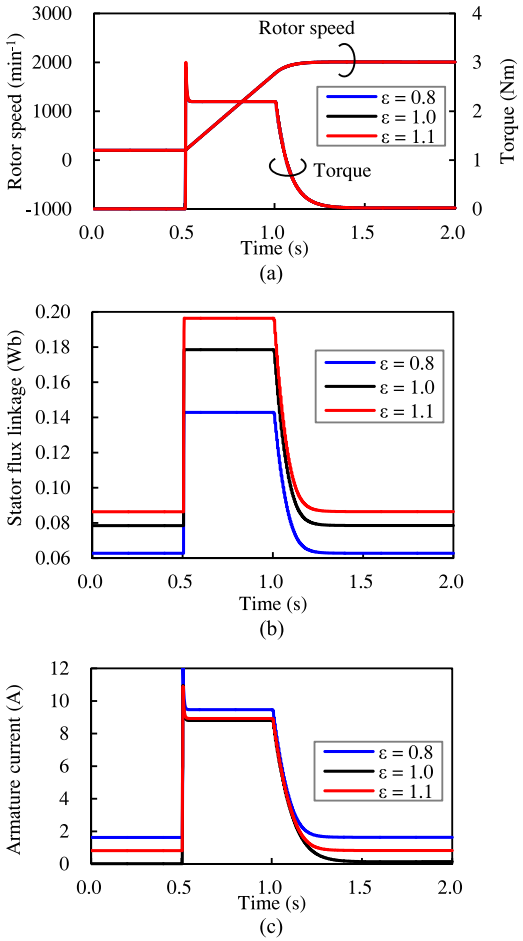

Fig. 8. Simulation results of the acceleration characteristics belonging to the correction rate ε. (a) Rotor speed and torque, (b) stator flux linkage, and (c) armature current.

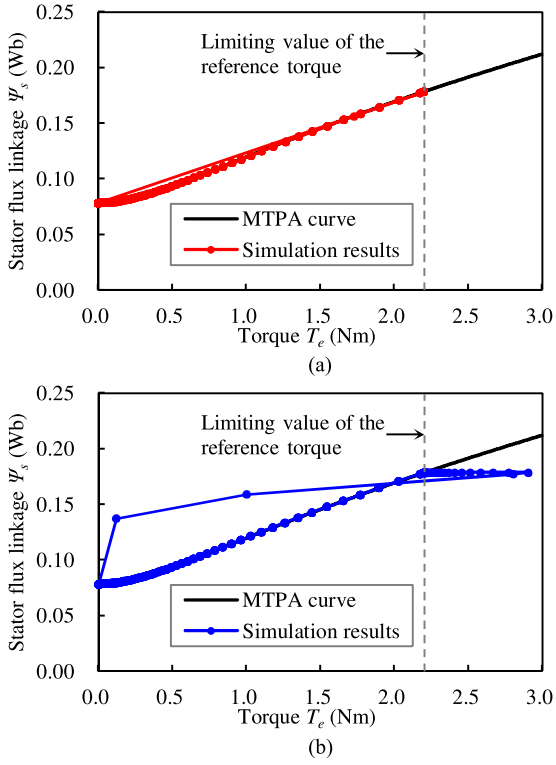

Fig. 9. Relationship between the torque and the stator flux linkage in acceleration in the case of $\varepsilon = 1$. (a) Reference value and (b) actual value.

D. Influence of Resistance Variations

The influence of armature resistance variations on MTPA control is discussed in this section. The variation of armature resistance is considered as the mismatched armature resistance value in controller. Motor 1 is applied to the tested system. To compare the effect of the errors of R_a, three cases are compared

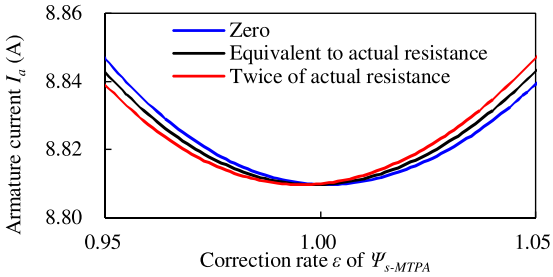

Fig. 10. Influence of the armature resistance in RFVC DTC with Motor 1 at the rotor speed of 300 min^{-1} and the load torque of 2.2 N · m.

about R_a:R_a in Fig. 5 sets zero, equivalent to actual value, or twice of actual value. In these simulations, the flux estimation is supposed to be accurate because of the stability of the DTC systems. The correction rate ε is added in a similar manner as the previous simulations.

Fig. 10 shows the relationship between I_a and ε under the rotor speed of 300 min^{-1} and the load of 2.2 N · m. In Fig. 10, the blue, black, and red lines are the case of applying zero, equivalent to actual R_a, and twice of actual R_a, respectively. The MTPA operating point is moved by the error of R_a. These results are estimated to be caused that the $\boldsymbol{v}_o^*$ generated from RFVC composes the error of voltage drop of armature resistance, and that the optimal $\boldsymbol{v}_a^*$ for MTPA control cannot be generated from optimal $\boldsymbol{\Psi}_s^*$ for MTPA control. Therefore, the optimal reference stator flux linkage for MTPA control is changed. For example, optimal reference flux increases when actual armature resistance increases with increase in temperature and the resistance in DTC keeps constant. However, the reference flux linkage is close to optimal value as shown in Fig. 10.

For the tested motor, the optimal reference flux linkage is little influenced by the armature resistance variations.

E. Influence of Inductance Variations

The influence of inductance variations on MTPA control is discussed in this section. Motor 2 is applied to the tested system. L_q is modeled as the function of i_q to assume inductance variation due to magnetic saturation. To compare the effect of inductance estimation, two cases are compared about L_q used for MTPA control: one is applying constant L_q and another is applying estimated L_q with twice iterated calculation in Fig. 4. The correction rate ε is added in a similar manner as the previous simulations.

Fig. 11 shows the relationship between I_a and ε under the rotor speed of 300 min^{-1}. In each graph, the blue line is the case of applying constant L_q (none of iterated calculation) and the red line is the case of applying estimated L_q with twice iterated calculation. The value of ε that satisfies the MTPA point is below 1 with constant L_q. Note that $\varepsilon < 1$ means that decreasing q-axis inductances cause a decrease in optimal flux linkage during MTPA operation. On the other hand, the MTPA control points are near $\varepsilon = 1$ when L_q is estimated by twice iterated calculation. As a result, it is necessary to consider inductance variations when the magnetic saturation cannot be neglected.

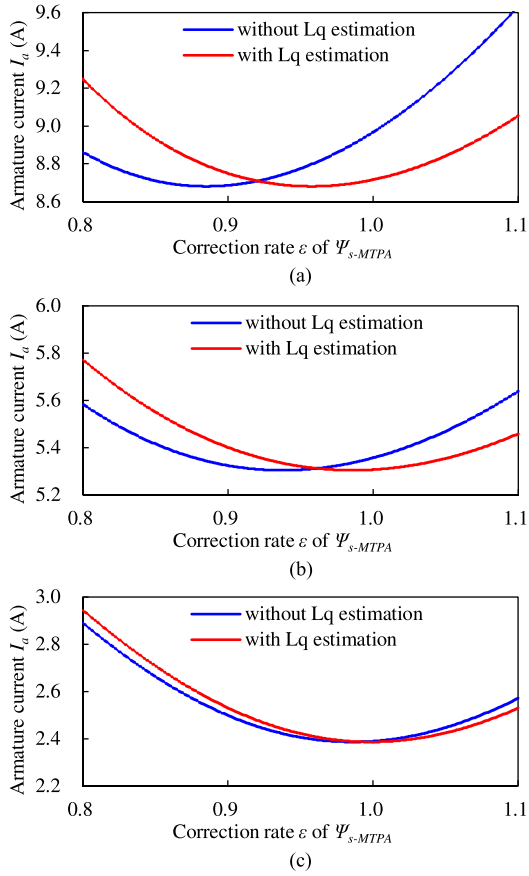

Fig. 11. Influence of the iterated calculation to the relationship between the armature current and the correction rate under the constant torque with Motor 2 at the rotor speed of 300 min-1: comparing none of and twice of inductance estimation (300 min^{-1}). (a) 1.8 N · m (rated), (b) 1.0 N · m, and (c) 0.4 N · m.

IV. Experimental Results

A. Tested System

The system shown in Fig. 5 is applied in the experiment in similar manner as in the simulation, along with Motor 2, and an insulated gate bipolar transistor inverter. The dc link voltage is 150 V. An eddy-current break is applied as the load. The carrier-based PWM is used in PWM inverter. All the controls were processed through a digital signal processor (Texas Instruments TMS320C6713). The parameters of the controller are shown in Table II. The proposed method is computed in a reference calculator with a control period of 5 ms.

In experiments, the stator flux linkage is estimated using (2) in d-q frame as shown in Fig. 12 to avoid variations of flux estimation error according to rotor speed or voltage frequency because the pure integrator based on (17) cannot be realized practically and the improved flux linkage estimators have dependency on the speed or on the voltage frequency [21], [23], [24], which are sensitive to the voltage offset errors.

B. Influence of Iterated Calculation

The influence of iterated calculation is discussed in this section. First, the relationship between ε and I_a under constant torque is verified in a similar manner as Fig. 11. The rotor speed

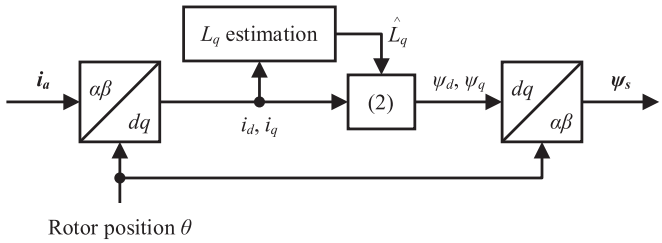

Fig. 12. Block diagram of the flux estimator in experiment.

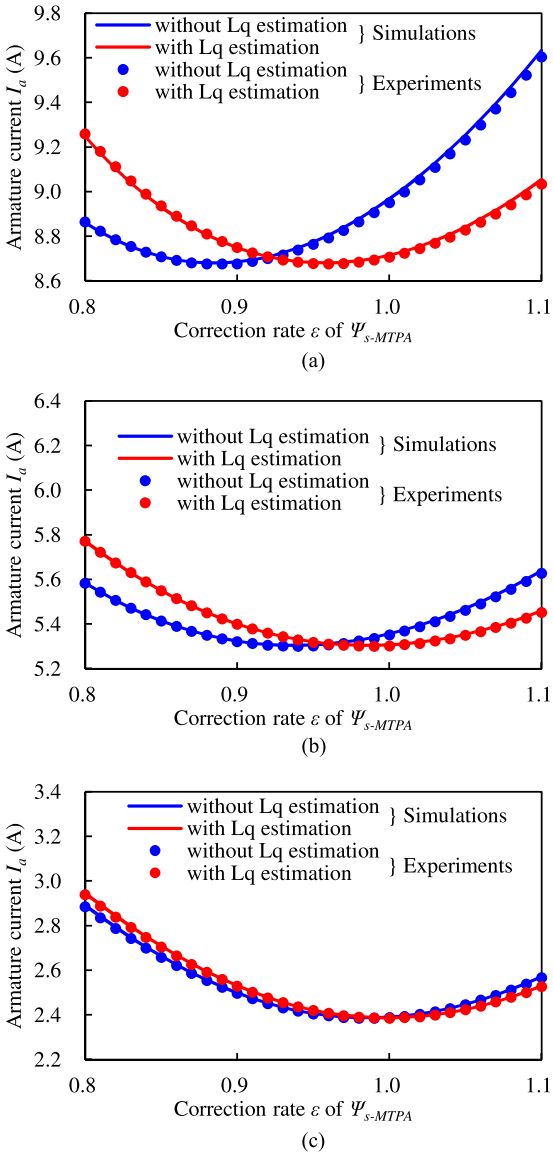

Fig. 13. Experimental results of the relationship between the armature current and the correction rate under the constant torque at the rotor speed of 300 min^{-1}: comparing none of and twice of inductance estimation. (a) 1.8 N · m (rated), (b) 1.0 N · m, and (c) 0.4 N · m.

is 300 min^{-1}, and the reference torque is set at 0.4, 1.0, and 1.6 N · m. Fig. 13 shows the experimental results and simulation results, and the experimental results agree with the simulation results.

Next, number of the iterations, calculation load, and the accuracy of MTPA condition are evaluated. Fig. 14 shows the effects

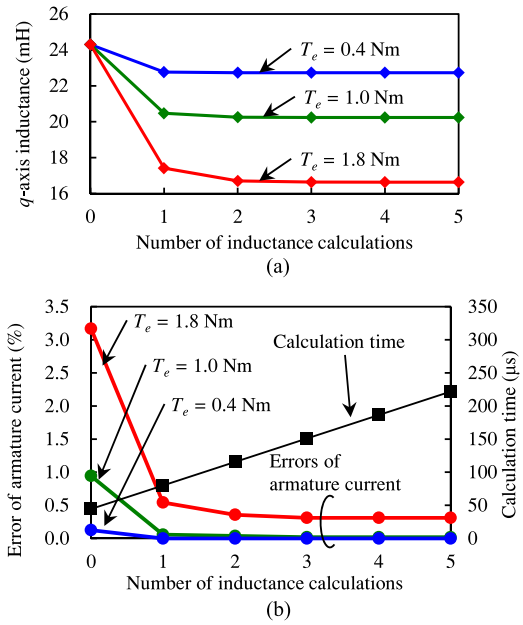

Fig. 14. Effect of the iteration of inductance calculation in the proposed method. (a) q-axis inductance value and (b) error of armature current and the calculation time.

of the number of the inductance calculations. The left of vertical axis in Fig. 14(b) means the error rate when $\varepsilon = 1$ to the current in MTPA condition. Increasing the number of the iterations decrease the q-axis inductance and the armature current. However, this also increase the calculation time of the proposed method, and the error to optimal current does not converge to zero as in the case of $T_e = 1.8$ N · m. Thus, a number of iterations for calculation should be considered. In this case, q-axis inductance is little change more than twice of inductance calculations as shown in Fig. 14(a). Thus, the error of armature current to optimal current decreases little. However, the error reduces to less than 0.5% with the iterated calculation. From this viewpoint, the number of the inductance calculation times should be twice for Motor 2.

C. Transient State

Fig. 15 shows the experimentally observed acceleration characteristics. The reference speed is changed from 200 to 2000 min^{-1} at 0.1 s. The reference torque is limited to 1.8 N · m, and the MTPA control is applied every time. To verify the proposed method, the correction rate ε is set at 0.8, 1.0, and 1.1. Fig. 15(a)–(d) show the rotor speed, estimated torque, estimated stator flux linkage, and armature current, respectively. Because of the limiting of the reference torque, the characteristics of the rotor speed and the estimated torque are very similar as shown in Fig. 15(a) and (b). However, the characteristics of the armature current are not similar because of the difference of the estimated flux linkage, as shown in Fig. 15(c) and (d), which is the same as the simulation results in Fig. 8. To compare three cases, the armature current is the smallest when $\varepsilon = 1$. Thus, the proposed method can generate appropriate reference flux linkage for MTPA control.

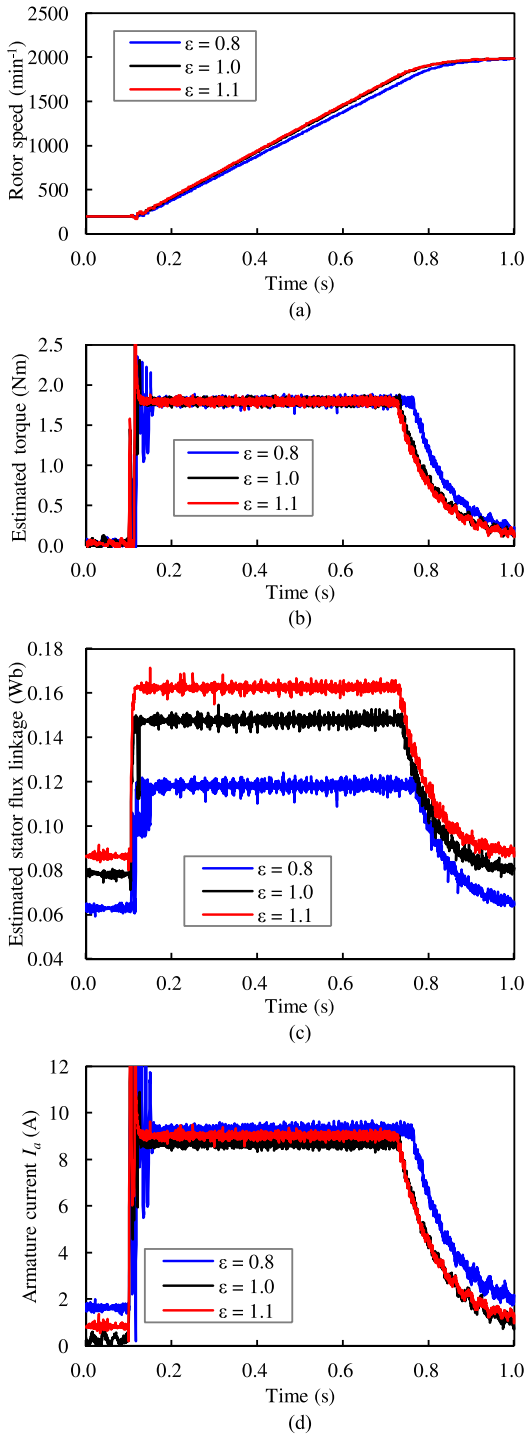

Fig. 15. Experimental results of the acceleration characteristics belonging to the correction rate ε. (a) Rotor speed, (b) estimated torque, (c) estimated stator flux linkage, and (d) armature current.

Fig. 16 shows the relationship between the torque and the stator flux linkage. The relationship follows the MTPA operating curve of the theoretical values regardless of the operating condition.

These results mean that $\Psi_{s\text{-}MTPA}$ with the proposed method can be applied in a transient state.

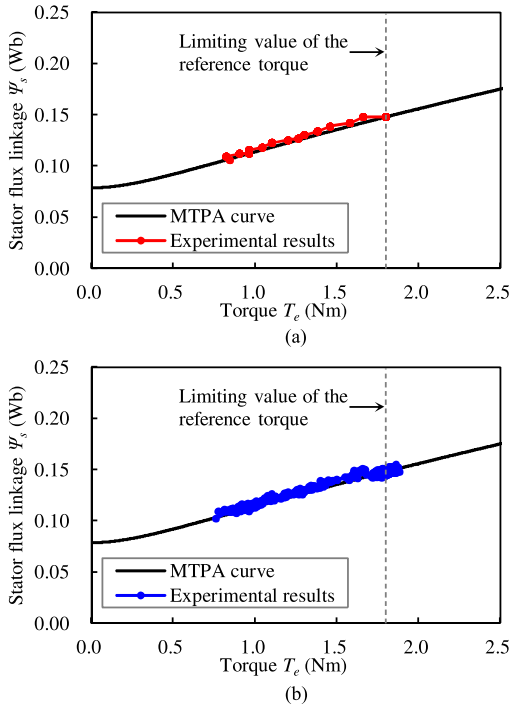

Fig. 16. Relationship between the torque and the stator flux linkage in acceleration in the case of $\varepsilon = 1$. (a) Reference value and (b) estimated value.

V. Conclusion

A reference flux linkage calculation method that can realize MTPA control for DTC-based IPMSM drives was proposed in this paper. The key features of the proposed method are that it is independent of the motor condition, excludes a parameter-dependent LUT, and provides accuracy improvement with iterated calculation techniques.

Simulation and experimental results show that the proposed method obtains the MTPA condition.

In this paper, inductance variation is duty considered when the inductances are modeled as functions of the current. Other estimation methods of inductance are also applied to the proposed system. Further, the proposed method can apply to any IPMSM drive system, whose references are the torque and stator flux linkages. In addition, the proposed method can be applied fully sensorless DTC system because the MTPA control strategy requires neither rotor position nor rotor speed.

Acknowledgment

This paper is the extension of the conference paper of [19].

References

[1] T. M. Jahns, B. K. Gerald, and W. N. Thomas, "Interior permanent magnet synchronous motors for adjustable speed drives," *IEEE Trans. Ind. Appl.*, vol. IA-22, no. 4, pp. 738–747, Jul./Aug. 1986.

[2] S. Morimoto, M. Sanada, and Y. Takeda, "Wide-speed operation of interior permanent magnet synchronous motors with high performance current regulator," *IEEE Trans. Ind. Appl.*, vol. 30, no. 4, pp. 920–926, Jul./Aug. 1994.

[3] Y. A.-R. I. Mohamed and T. K. Lee, "Adaptive self-turning MTPA vector controller for IPMSM drive system," *IEEE Trans. Energy Convers.*, vol. 21, no. 3, pp. 636–644, Sep. 2006.

[4] P. Niazi, A. Toliyat, and A. Goodarzi, "Robust maximum torque per ampere (MTPA) control of PM-Assisted SynRM for traction applications," *IEEE Trans. Veh. Technol.*, vol. 56, no. 4, pp. 1538–1545, Jul. 2007.
[5] A. Consoli, G. Scarcella, G. Scelba, and A. Testa, "Steady-state and transient operation of IPMSMs under maximum-torque-per-ampere control," *IEEE Trans. Ind. Appl.*, vol. 46, no. 1, pp. 121–129, Jan./Feb. 2010.
[6] S. Kim, Y.-D. Yoon, S.-K. Sul, and K. Ide, "Maximum torque per ampere (MTPA) control of an IPM machine based on signal injection considering inductance saturation," *IEEE Trans. Power Electron.*, vol. 28, no. 1, pp. 488–497, Jan. 2013.
[7] E. Daryabeigi, H. A. Zarchi, G. R. A. Markadeh, J. Soltani, and F. Blaabjerg, "Online MTPA control approach for synchronous reluctance motor drives based on emotional controller," *IEEE Trans. Power Electron.*, vol. 30, no. 4, pp. 2157–2166, Apr. 2015.
[8] M. Preindl and S. Bolognani, "Optimal state reference computation with constrained MTPA criterion for PM motor drives," *IEEE Trans. Power Electron.*, vol. 30, no. 8, pp. 4524–4535, Aug. 2015.
[9] T. Sun and J. Wang, "Extension of virtual-signal-injection-based MTPA control for interior permanent magnet synchronous machine drives into the field-weakening region," *IEEE Trans. Ind. Electron.*, vol. 62, no. 11, pp. 6809–6817, Nov. 2015.
[10] I. Takahashi and T. Noguchi, "A new quick-response and high-efficiency control strategy of an induction motor," *IEEE Trans. Ind. Appl.*, vol. IA-22, no. 5, pp. 820–827, Sep. 1986.
[11] M. F. Rahman, L. Zhong, and K. W. Lim, "A direct torque-controlled interior permanent magnet synchronous motor drive incorporating field weakening," *IEEE Trans. Ind. Appl.*, vol. 34, no. 6, pp. 1246–1253, Nov./Dec. 1998.
[12] G. S. Buja and M. P. Kazmierkowski, "Direct torque control of PWM inverter-fed AC motors - A survey," *IEEE Trans. Ind. Electron.*, vol. 51, no. 4, pp. 744–757, Aug. 2004.
[13] Y. Inoue, S. Morimoto, and M. Sanada, "A novel control scheme for maximum power operation of synchronous reluctance motors including maximum torque per flux control," *IEEE Trans. Ind. Appl.*, vol. 47, no. 1, pp. 115–121, Jan./Feb. 2011.
[14] S. Bolognani, L. Peretti, and M. Zigliotto, "Online MTPA control strategy for DTC synchronous-reluctance-motor drives," *IEEE Trans. Power Electron.*, vol. 26, no. 1, pp. 20–28, Jan. 2011.
[15] G. Foo, S. Sayeff, and M. F. Rahman, "Low-speed and standstill operation of a sensorless direct torque and flux controlled IPM synchronous motor drives," *IEEE Trans. Energy Convers.*, vol. 25, no. 1, pp. 25–33, Mar. 2010.
[16] M. Preindl and S. Bolognani, "Model predictive direct torque control with finite control set of PMSM drive systems, part 1: Maximum torque per ampere operation," *IEEE Trans. Ind. Inform.*, vol. 9, no. 4, pp. 1912–1921, Nov. 2013.
[17] T. Inoue, Y. Inoue, S. Morimoto, and M. Sanada, "Mathematical model for MTPA control of permanent-magnet synchronous motor in stator flux linkage synchronous frame," *IEEE Trans. Ind. Appl.*, vol. 51, no. 5, pp. 3620–3628, Sep./Oct. 2015.
[18] A. Shinohara, Y. Inoue, S. Morimoto, and M. Sanada. "Correction of reference flux for MTPA control in direct torque controlled interior permanent magnet synchronous motor drives," in *Proc. Int. Power Electron. Conf.*, May 2014, pp. 324–329.
[19] A. Shinohara, Y. Inoue, S. Morimoto, and M. Sanada, "A calculation method of reference flux to realize maximum torque per ampere control in direct torque controlled permanent magnet synchronous motor drives," in *Proc. 10th IEEE Int. Conf. Power Electron. Drive Syst.*, Apr. 2013, pp. 205–210.
[20] I. Boldea, M. C. Paicu, and G.-D. Andreescu, "Active flux concept for motion-sensorless unified AC motor," *IEEE Trans. Power Electron.*, vol. 23, no. 5, pp. 2612–2618, Sep. 2008.
[21] G. H. B. Foo and M. F. Rahman, "Direct torque control of an IPM-synchronous motor drive at very low speed using a sliding-mode stator flux observer," *IEEE Trans. Power Electron.*, vol. 25, no. 4, pp. 933–942, Apr. 2010.
[22] L.Tang, L. Zhong, M. F. Rahman, and Y. Hu, "A novel direct torque controlled interior permanent magnet synchronous machine drive with low ripple in flux and torque and fixed switching frequency," *IEEE Trans. Power Electron.*, vol. 19, no. 2, pp. 346–356, Mar. 2004.
[23] D. Stojić, M. Milinković, S. Veinović, and I. Klasnić, "Improved stator flux estimator for speed sensorless induction motor drives," *IEEE Trans. Power Electron.*, vol. 30, no. 4, pp. 2363–2371, Apr. 2015.
[24] A. Shinohara, Y. Inoue, S. Morimoto, and M. Sanada, "Comparison of stator flux linkage estimators for PWM-based direct torque controlled PMSM drives," in *Proc. 11th IEEE Int. Conf. Power Electron. Drive Syst.*, Jun. 2015, pp. 1035–1040.

Atsushi Shinohara (S'15) received the B.E. and M.E. degrees from Osaka Prefecture University, Sakai, Japan, in 2012 and 2014, respectively. He is currently working toward the Ph.D. degree in the Department of Electrical and Information Systems, Graduate School of Engineering, Osaka Prefecture University, Sakai, Japan.

His research interests include control of electrical drives of synchronous motors.

Mr. Shinohara is a member of the Institute of Electrical Engineers of Japan.

Yukinori Inoue (S'07–M'10) received the B.E., M.E., and Ph.D. degrees from Osaka Prefecture University, Sakai, Japan, in 2005, 2007, and 2010, respectively.

Since 2010, he has been with the Graduate School of Engineering, Osaka Prefecture University, where he is currently an Associate Professor. His research interests include control of electrical drives, particularly the direct torque control of permanent-magnet synchronous motors and position-sensorless control of these motors.

Dr. Inoue is a member of the Institute of Electrical Engineers of Japan, and the Japan Institute of Power Electronics.

Shigeo Morimoto (M'93) received the B.E., M.E., and Ph.D. degrees from Osaka Prefecture University, Sakai, Japan, in 1982, 1984, and 1990, respectively.

In 1984, he joined Mitsubishi Electric Corporation, Amagasaki, Japan. Since 1988, he has been with the Graduate School of Engineering, Osaka Prefecture University, where he is currently a Professor.

His main areas of research interest are permanent magnet synchronous machines, reluctance machines and their control systems.

Dr. Morimoto is a member of the Institute of Electrical Engineers of Japan, the Society of Instrument and Control Engineers of Japan, the Institute of Systems, Control and Information Engineers, and the Japan Institute of Power Electronics.

Masayuki Sanada (M'94) received the B.E., M.E., and Ph.D. degrees from Osaka Prefecture University, Sakai, Japan, in 1989, 1991, and 1994, respectively.

Since 1994, he has been with the Graduate School of Engineering, Osaka Prefecture University, where he is currently an Associate Professor. His main areas of research interest are permanent- magnet motors for direct-drive applications, their control systems, and magnetic field analysis.

Dr. Sanada is a member of the Institute of Electrical Engineers of Japan, the Japan Institute of Power Electronics, and the Japan Society of Applied Electromagnetics and Mechanics.